A NOVEL DESIGN METHOD OF VARIABLE GEOMETRY TURBINE NOZZLES FOR HIGH EXPANSION RATIOS

Lei Huang[1], Hua Chen[2,*]

1. National Laboratory of Engine Turbocharging Technology, North China Engine Research Institute, 96 Yongjin Road, Beichen District, Tianjin, China 300400

2. Dalian Maritime University, 1 Linghai Road, Dalian, China 116026

**Corresponding author. Tel.:+86-135-0205-7256, E-mail:huachen204887@163.com*

Abstract

In variable nozzle geometry turbines (VNT), opening of the nozzles is used to control turbine mass flow and expansion ratio, allowing more turbine power to be generated over wider operating conditions. In turbocharged vehicles, the nozzles are 'closed' to provide high boosts for engine and vehicle acceleration and for engine braking assistance. At the both conditions, high nozzle expansion ratios are created, and shockwaves may generate from the nozzles. These shocks reduce turbine efficiency and they can cause high cycle fatigue (HCF) damage to the downstream rotor blades. Design of high expansion ratio radial nozzles is difficult for VNT because transonic flows are very sensitive to small geometry changes, and the large semi-vaneless space created by the nozzles makes the design a tricky business. Shock minimised nozzle designs are therefore often achieved by auto-optimisation technique. While design targets may be achieved, this technique does not offer sufficient insights into how the optimal flow field has been derived, so the same optimisation procedure has to be applied to every new design. In this paper, a new design method that overcomes this problem is proposed. The method first uses a conformal mapping to transfer a radial nozzle from the r-θ plane into the x-y plane. Mapped nozzle displays amplification of supersonic acceleration and diffusion. This is explained by the curvature changes brought about by the mapping, and a link between the shock strength and the flatness of the suction surface of the mapped nozzle is found. The amplification and the link can be utilised to design nozzles with reduced shock loss in the x-y plane first and then mapped back to the r-θ plane. Two nozzles for 6:1 expansion ratio were designed in this way and CFD results show a significant reduction of nozzle loss. The nozzles were also checked for fully open condition and no performance penalty was found.

Keywords

turbine nozzle, aerodynamic design, conformal mapping

Nomenclature

CFD	Computational fluid dynamics
HCF	High cycle fatigue
VNT	Variable nozzle turbine
r	Radius, radial coordinate
p	Pressure
x, y	Cartesian coordinates
θ	Azimuth angle

Subscript

0	Total stage
1	Inlet
2	Outlet
Ref	Referential

1. Introduction

The turbine of a vehicle turbocharger is subject to a wide flow range and demanding power requirements. At low mass flows, high efficiency and power output are required to improve engine torque and transient response, while a high flow capacity is needed for engine rated power and to reduce engine pumping loss at high speeds. To meet these challenging needs, variable Nozzle Turbines (VNT) employ a nozzle ring upstream of the rotor, by changing the setting angle of the nozzle vanes, different values of nozzle throat area and vane exit angle can be achieved. When an acceleration of the engine or turbine is required, the nozzles are closed to reduce the throat area and make the nozzle exit flow more tangential. So a higher nozzle exit velocity is achieved in a more tangential direction, which enables the rotor to produce more Euler's work. Closing the nozzles can also be used for engine deceleration or braking purpose. This increases the pressure expansion ratio across the nozzles and establishes a high back pressure at engine exhaust manifold, adding to the pumping loss of the engine.

When the flow inside the nozzles of a VNT turbine is subsonic or the expansion ratio of the nozzles is well below 2, geometry of the nozzles matters little to the flow loss within the nozzles. When the expansion ≥ 2, the flow in parts of the nozzles may becomes supersonic, and shockwaves could generate from nozzles. Such expansion ratios exist at engine braking or during unconstrained turbine acceleration. **Figure 1** shows calculated Mach no. of a VNT nozzle ring under such a condition, shockwaves generated from the underside or suction side of the nozzles are visible.

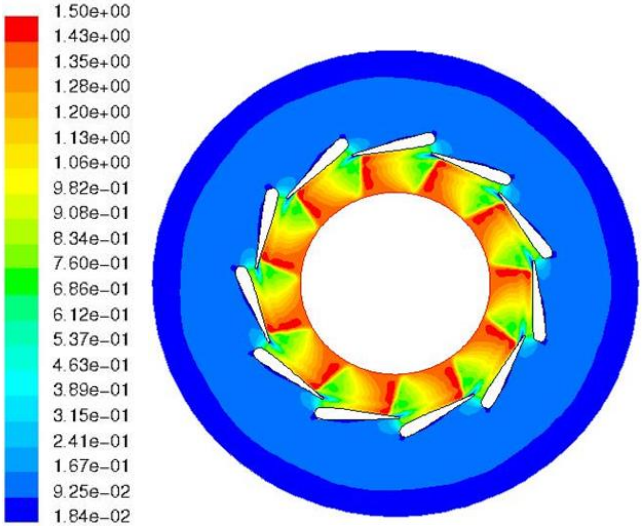

Fig. 1 Calculated Mach no. of a VNT nozzle ring under a high expansion ratio [1]

These shocks generate losses and reduce turbine efficiency. They will also interact with the downstream rotor and can cause HCF of the rotor blades. The HCF is one of the major concerns in VNT rotor design [2]. Efforts were made to design VNT nozzles so that they generate no or weaker shocks and have less losses. Yang et al. [3] proposed an increase of nozzle vane number to provide better guidance to the flow to reduce shock strength. This method however increases nozzle surface friction loss, which is often unacceptable. Zhao et al. [4] suggested adding grooves to the suction surface of the vanes, and their simulation showed that the shocks were weakened and rotor excitation was reduced by 30%, but the nozzle loss was increased. These references dealt with thick vanes used in Honeywell's AVNT, a special type of VNTs

that requires thick nozzle vanes. For ordinary VNTs that accept thinner vanes, the optimum vane geometry can and was obtained through auto-optimisation technique [1]. A geometry generating tool coupled with CFD code and driven by an optimisation software was able to generate a geometry that minimises the shock and significantly reduces flow losses. One of such an example is given in **Figure 2**. It can be seen that the suction side diffusion is minimised.

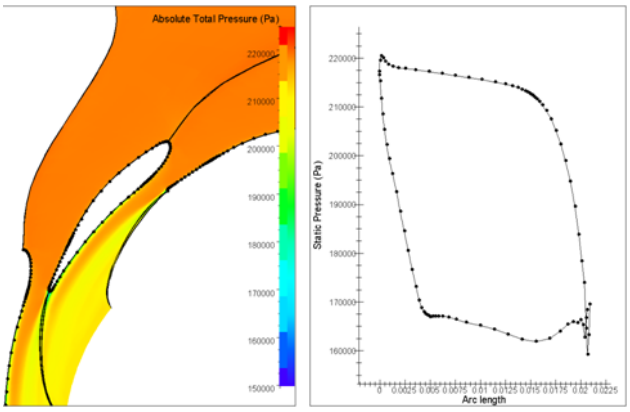

Fig. 2 Calculated total pressure distribution (left) and static pressure loading (right) of an optimised VNT nozzle

While the auto-optimisation method is capable of producing optimal designs, they offer little insights as why a particular geometry is better than others, or how the optimal flow such as the vane loading shown in **Figure 2** is linked to the geometry in the same figure. One of the difficulty in design of radial nozzles for turbocharger VNTs is that the adjacent pair of nozzle vanes usually do not form a proper 'nozzle' in the sense that a large part of the flow region is so called semi-vaneless space (See **Figure 1**). The auto-optimisation technique does not provide a clear design guideline for this region, thereby every new nozzle must be designed using the same black box procedure.

In this paper, we put forward a new design methodology for VNT nozzles that can show clearly the relationship between vane geometry and flow physics, and so can provide design guidelines. It can produce similarly good designs with low losses and weak HCF excitations as the auto-optimisation. We demonstrate these through an example of improving an existing nozzle designed by the auto-optimisation.

2. The methodology and its application

2.1 The baseline nozzle

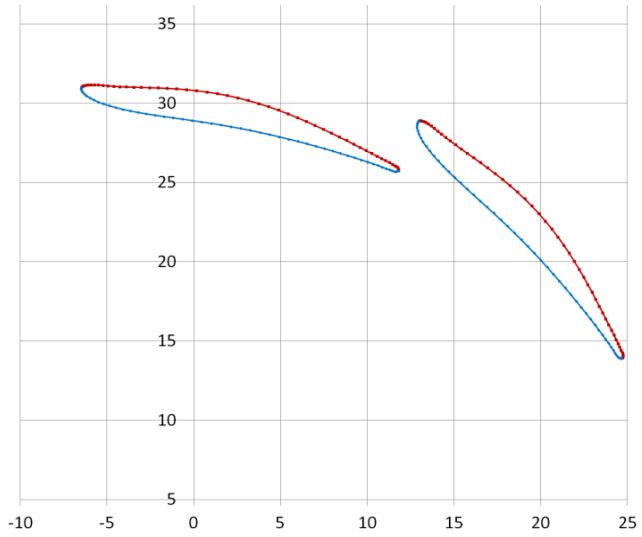

a) Geometry

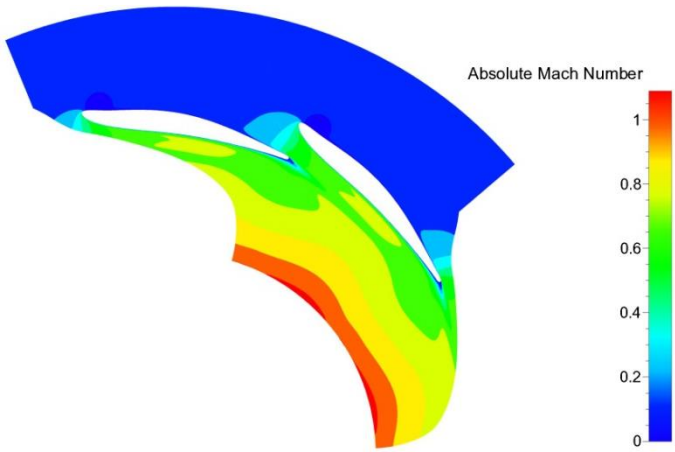

b) Predicted Mach no. distribution

Fig. 3 Baseline VNT nozzle and Mach number distribution at expansion ratio 2:1

The baseline nozzle to be improved is a VNT nozzle for automotive application which was designed using the auto-optimisation technique mentioned earlier. **Figure 3a** shows the nozzle at a closed position and **Figure 3b** gives predict-

ed Mach no. distribution at this position and an expansion ratio of 2:1.

The computation that produced this result and others followed was carried out with commercial software Fineturbo in which 2D Navier-Stokes equations were solved with the Spalart-Allmaras turbulence closure. Turbine housing and turbine wheel were not included in the calculation, they merely proved the inlet and outlet boundaries. The term of expansion ratio here and afterward refers to the total-to-static pressure ratio across the computational domain, and not the turbine stage. When the nozzle is closed at low rotor speeds, the mass flow of the turbine stage is small. In this condition the pressure drop across the rotor is small with the most of stage pressure drop happens inside the nozzle. On the other hand, when the nozzle is open at high rotor speeds, the mass flow of the stage is larger and so is the pressure drop of the rotor. In this condition, nozzle expansion ratio is a smaller portion of the stage expansion ratio.

Although there is a flow acceleration after geometric throat of the nozzle in the semi-vaneless space along the suction side, the entire flow is subsonic therefore no shocks are produced. There is a small flow diffusion after the acceleration toward vane trailing edge, in order that both the pressure side and the suction side have the same pressure when they meet at the edge. This small diffusion can also be seen in **Figure 2**. Our design target is a new nozzle that maintains this level of performance at this expansion ratio, while improves upon it at higher expansion ratios when the turbine is in engine braking mode.

2.2 Conformal mapping

The nozzle has a long semi-vaneless space, and the radial inflow nature of the nozzle makes it difficult to gauge the flow area variation after the nozzle throat and other key geometric features that may affect the flow. So a conformal mapping was first carried out to map the nozzle from the r-θ plane into the x-y plane,

$$\theta = x / r_{ref}, \quad \frac{r}{r_{ref}} = e^{y/r_{ref}} \qquad (1)$$

where r_{ref} is a reference radius, and r_{ref} was taken here as the mean of the maximum and minimum radii of the nozzle. This type of conformal mapping has been used in compressor diffuser vane design [5], and is also used by other industries in radial turbine nozzle design [6]. Mapped nozzle is shown in **Figure 4a**, and CFD predicted Mach no. distribution at the same expansion ratio of 2:1 for this mapped nozzle is given in **Figure 4b**. While no shock exists before the mapping, a shock is now generated from the suction side of the nozzle vane after the mapping. At the first glance, this result seems to suggest that the conformal mapping may not be useful because it does not reproduce the original flow field.

Since eq. (1) is a conformal mapping, the vane angle of the nozzle in **Figure 3**a is kept in **Figure 4a**, and this is a useful feature of the conformal mapping. Surface length of the nozzle vanes on the other hand is not maintained after the mapping, and this mainly produces the discrepancy of the flow field. Using eq. (1), the relationship between the total differentials of any surface length in the two mapping planes can be obtained,

$$ds_{x-y} = \left(\frac{r_{ref}}{r} \right) ds_{r-\theta} \qquad (2)$$

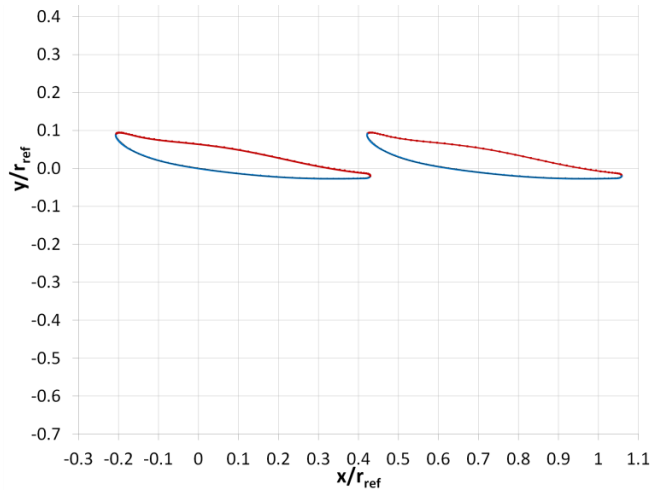

a) Geometry

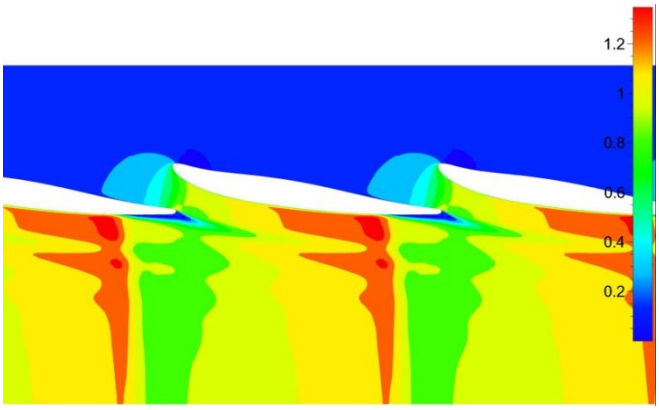

b) Predicted Mach no. distribution

Fig. 4 Geometry and Mach number distribution of the baseline nozzle at expansion ratio 2:1 after conformal mapping of eq. (1)

It can be seen from eq. (2) that only when $r = r_{ref}$ or $y/r_{ref} = 0$ the two total differentials are equal. Because vane surface angle is kept the same after the mapping, this means that the rate of the angle changes along the nozzle surfaces or nozzle surface curvature is only equal in the two mapping planes when $r = r_{ref}$ or $y/r_{ref} = 0$, otherwise they are different. When $r > r_{ref}$, $ds_{x\text{-}y} < ds_{r\text{-}q}$, the vane angle change in the x-y plane will be larger or quicker than in the r-θ plane and vice versa. Choice of r_{ref} in the mapping therefore affects vane surface curvature and flow behaviour in the x-y plane. In this case, the choice of r_{ref} results in a quicker vane turning in the first part of the suction surface from vane leading edge to $y/r_{ref} = 0$ (Figure 4a), and a slower vane turning afterwards. The rapid turning before the throat in the x-y nozzle almost chokes the nozzle at the throat. After the throat, the flow continuously accelerates along the convex suction surface and becomes supersonic until a shock is formed to meet trailing edge pressure rise condition. While the r-θ nozzle does not choke at its throat, further subsonic acceleration happens after the throat.

The blade static pressure loading is compared for the two nozzles in **Figure 5**. It further shows the influence of vane turning rate. According to eq. (2) the largest increase of the vane turning rate happens at the leading edge where r is the largest of the entire suction surface, this led to a large flow acceleration around the leading edge in the mapped nozzle.

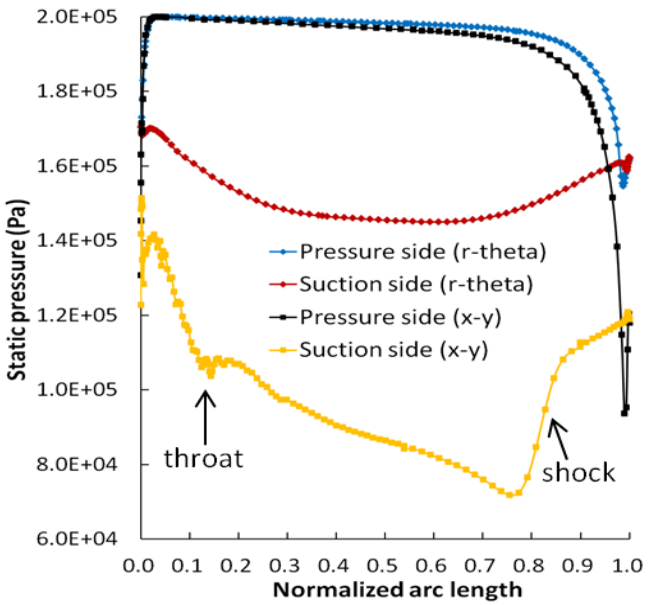

Fig. 5 Comparison of loading for vanes before and after the conformal mapping, nozzle expansion ratio = 2:1

2.3 Optimisation of the nozzle in the x-y plane

Looking at **Figure 5**, one sees that in the both nozzles, flow along the suction first accelerates and then diffuses. The only difference seems to be that the one after the mapping displays much stronger acceleration and deceleration due to the reason explained above. This suggests that if a nozzle is optimised in the mapped x-y plan by controlling these accel-

eration and deceleration, it may work equally well when it is mapped back to the r-θ plane using the same conformal mapping. This interpolation of the CFD results offers a possible way to design radial nozzles, because working in the x-y plane is always easier than in the r-θ plane. One may also reason that when nozzle expansion ratio increases from current 2:1 to higher values, flow in the baseline nozzle (in the r-θ plane) may become similar to one shown in **Figure 4b**, that is, choking may happen near the throat followed by a supersonic acceleration along the suction surface which then ends with a shock. **Figure 6** shows the blade loading of the baseline nozzle when the pressure expansion ratio is 6:1. The similarity of the suction side loading is clear to that of the mapped nozzle in the x-y plane subject to 2:1 expansion ratio (yellow curve in **Figure 5**). This implies that to design a radial nozzle for high expansion rations, one may use the conformal mapping of eq. (1) and design it at a lower expansion ratio in the x-y plane.

To reduce the shock loss and the shock-related excitation, the supersonic acceleration in the semi-vanelss space needs to be reduced. Flow acceleration is controlled by two factors, the area schedule that affects mean flow velocity and surface curvature that influences local acceleration. The flow picture in **Figure 4b** provides some hints on how the passage area is seen by the flow in this space, and these will be looked into in future. Local flow acceleration is studied first because it provides a direct link between the geometry and the flow locally thus is useful in design optimisation. As will be seen later, the results justify this choice. In the x-y plane, a convex surface will produce local flow acceleration, and in this regard, the surface may be measured by the change of its first derivative. To reduce supersonic acceleration, a surface should be flat so the derivative of the surface should remain constant.

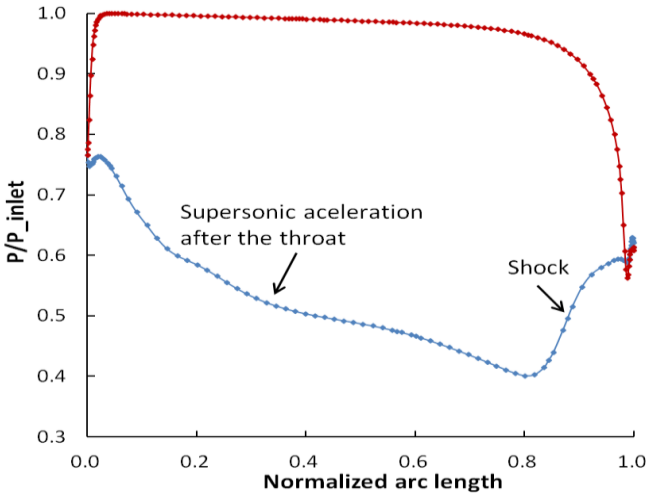

Fig. 6 Loading of baseline nozzle at 6:1 expansion ratio

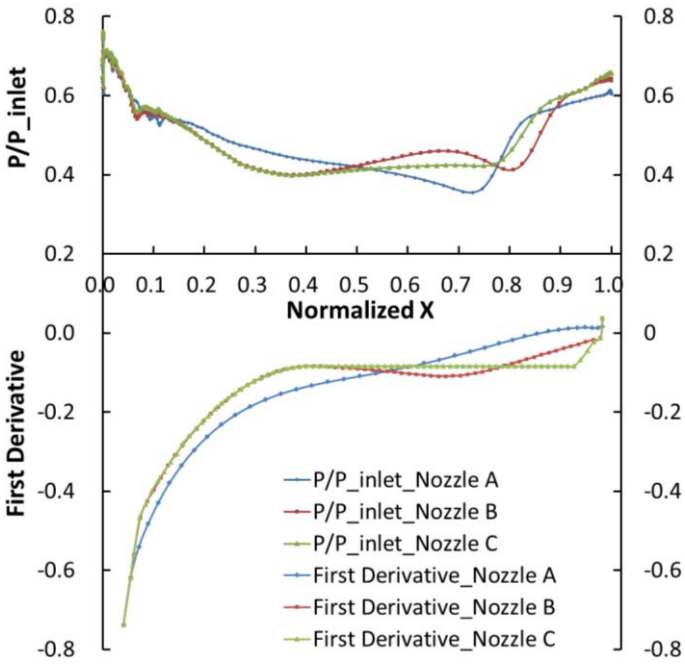

Fig. 7 Suction surface loading and surface derivative of three different x-y nozzles. Nozzle A is the mapped baseline. Nozzle expansion ratio = 2:1

Figure 7 compares the suction surface pressure loading and correspondent surface derivatives of three different x-y plane nozzles. Nozzle A is the mapped baseline nozzle with geometry given in **Figure 4a**. B and C are the two new designs trying to weaken the shock seen in Nozzle A by making the derivative curve as flat as possible after the throat in the supersonic acceleration region. A noticeable link be-

tween the flatness of the derivative and the pressure variation and the final pressure jump caused by the shock can be seen. The two new nozzles are shown to have better suction side loading patterns than that of baseline nozzle A. Shape of the three nozzles is compared in **Figure 8**, suction surface of the new nozzles is flatter than the baseline. In making the change to nozzle geometry, the geometric throat area of nozzle A was kept to minimise the effect to nozzle mass flow. Performance of the three nozzles under expansion ratio 2:1 is summarised in **Table 1**, which shows a large improvement to the loss coefficient by the two new nozzles.

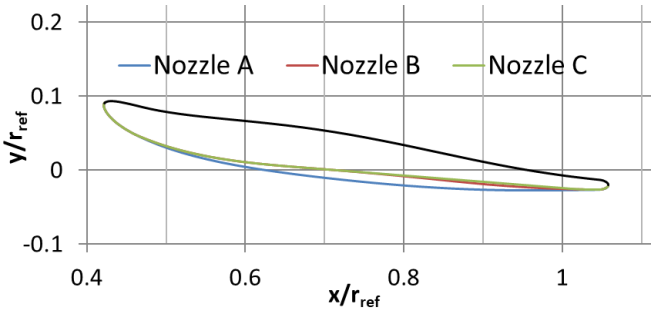

Fig. 8 Geometry of nozzles A, B and C in the x-y plane

Table 1 Performance of three nozzles in Figures 7 & 8

Nozzle	A	B	C
Loss coefficient =(p_{02}-p_2)/(p_{01}-p_2)	0.809	0.882	0.871
Relative mass flow	1.00	0.993	0.986

3. Results and discussion

The two new nozzles were mapped back to the r-θ plane by conformal mapping of eq. (1). **Figure 9** compares their geometry with the baseline's. While the suction surface of the new nozzles in the x-y plane is flatter than the baseline, **Figure 8**, they become curvier in the r-θ plane. Such a change is less intuitive if the geometry modification was carried out in the r-θ plane.

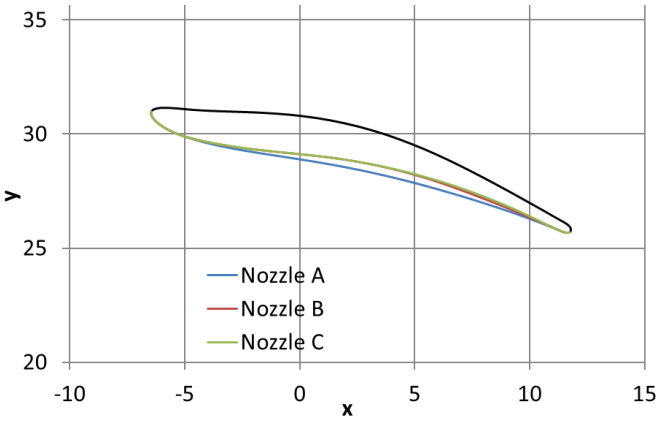

Fig. 9 Geometry of three nozzles in the r-θ plane

CFD was run to check the performance of the new nozzles against design objectives. **Figure 10** gives the results at several pressure expansion ratios. While keeping nearly the same mass flows as the baseline, the two new nozzles achieves reduced losses than the baseline, and this advantage increases with nozzle expansion ratio. The best Nozzle C achieves 7 points improvements in the loss coefficient over the baseline at expansion ratio 6:1. This may be compared with the gain of 6.2 points in the x-y plane at expansion ratio 2:1 in **Table 1**. The improvement come as the results of better suction side pressure loading, which is illustrated in **Figure 11** for expansion ratio 6:1 case. The expansion before the throat is similar for the three nozzles, but after the throat the flows in the new nozzles first accelerate, then change to a more or less constant pace (Nozzle C in particular), before a shock wave sets in. In comparison the flow in the baseline nozzle accelerates continuously without any pauses until a strong shock being produced. The circumferential variation of static pressure at nozzle exits is compared in **Figure 12** for the three nozzles. As can be seen from the Figure, the two new designs have reduced the jump caused by the shock.

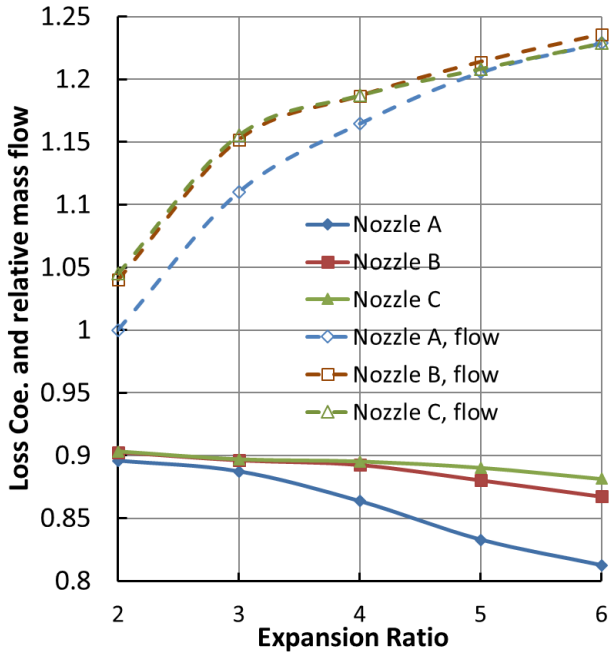

Fig. 10 Performance of new nozzles at high expansion ratios, nozzles are closed.

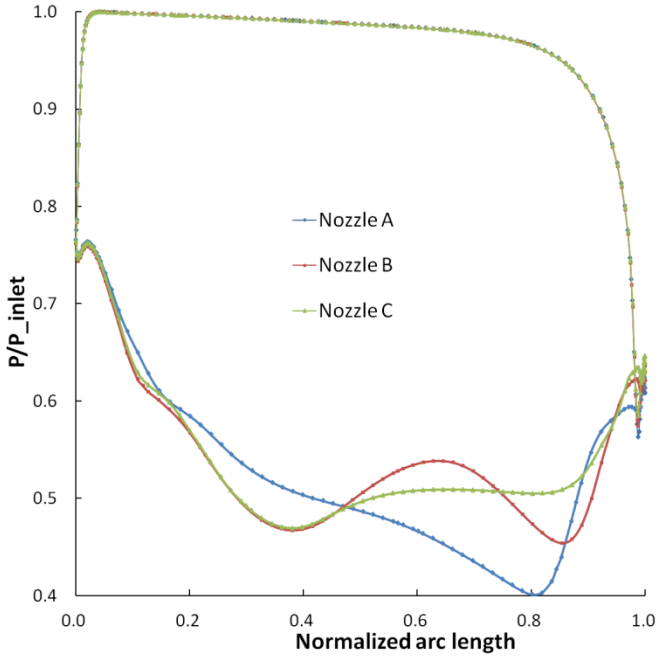

Fig. 11 Loading of three nozzles at expansion ratio 6:1, nozzles are closed.

VNT nozzles need to operate at different openings. So, the performance of the new nozzles at full opening were also checked by CFD. The geometry of the new and baseline nozzles at such opening is given in **Figure 13**. The CFD results are shown in **Figure 14**. When VNT nozzles are in fully opened position, the expansion ratio of the nozzles will be relatively small while the rotor takes a large portion of stage expansion ratio. Under small expansion ratios (≤ 2:1), the losses of the three nozzles, as expected, are largely the same. The new nozzles have slightly higher mass flow because of increased throat area.

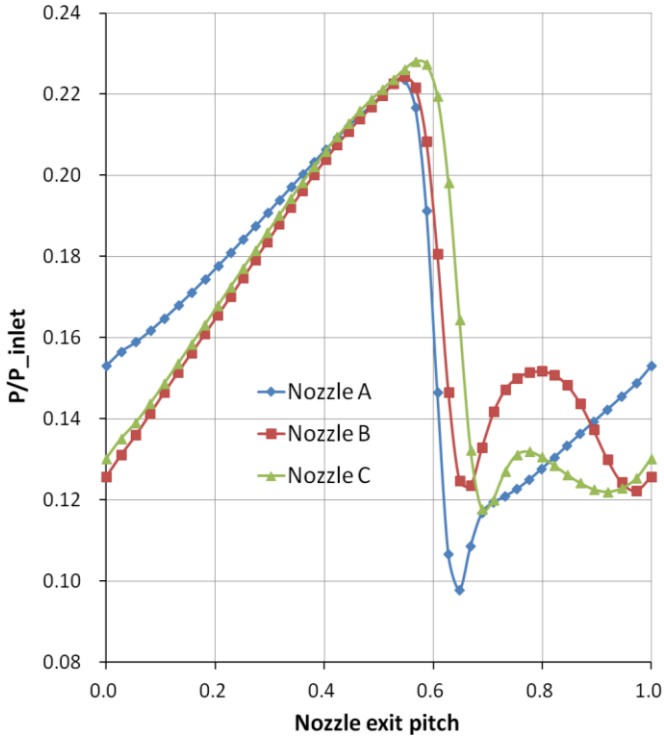

Fig. 12 Pressure variation at nozzle exit at expansion ratio 6:1, nozzles are closed.

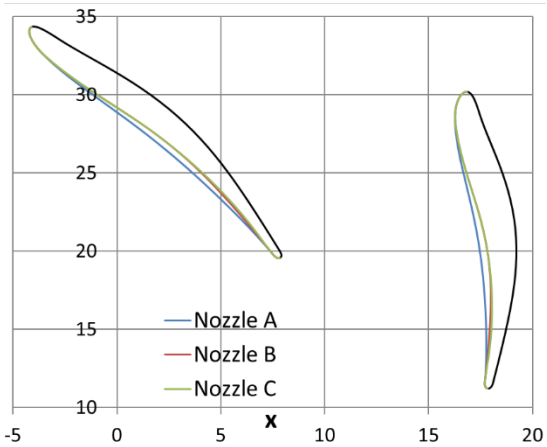

Fig. 13 Nozzles A, B and C in fully opened position

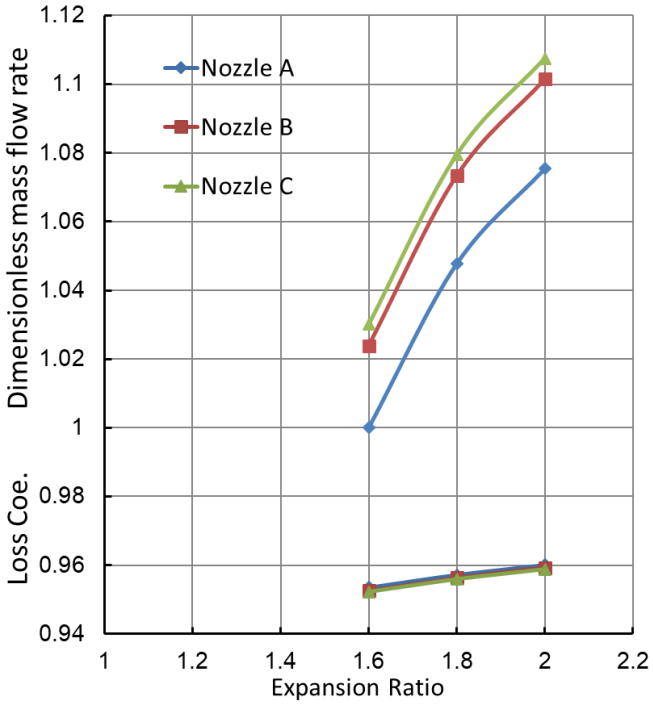

Fig. 14 Performance of three nozzles in fully opened position

4. Conclusions

A new design method of radial nozzles for high expansion ratios has been developed. It first uses conformal mapping of eq. (1) to map the nozzle geometry from the r-θ plane into the x-y plane then works with the nozzle in the x-y plane to optimise its geometry before mapping the nozzle back to the r-θ plane.

The total differentials of the correspondent nozzle surface arc length in the two planes of eq. (1) are linked through eq. (2), which can be used to explain the flow field variation before and after the mapping. When the mean radius of vanes is used as the reference radius in the mapping, the curvature of the front part of the suction surface is amplified and the rear part reduced. This creases a strong supersonic acceleration along the surface leading to a shock termination which would not happen in the r-θ plane under moderate expansion ratios. This suggests that should a nozzle in the x-y plane work well under these expansion ratios, it could work equally fine at higher expansion ratios after mapping to the r-θ plane.

The new method was applied to a VNT nozzle for automotive turbochargers, and two new nozzles were designed. By making the suction surface in the x-y plane flatter than the baseline nozzle after the throat, the new nozzles display less supersonic acceleration and weak shocks than the baseline. When mapped back to the r-θ plane, they both show better vane loadings, lower losses than and reduced exit pressure variations to the original nozzle which was previously designed by an auto-optimisation method for a slightly different operating condition.

Current method does not consider area effect after geometric throat. As flow is not fully choked at the throat under moderate expansion ratios, modification of suction surface geometry after the throat will affect aerodynamic throat area, and can change nozzle mass flow under such expansion ratios. This is an area of the new method to be improved. Second thing to be understood is why in the x-y plane, Nozzle B appears more efficient than Nozzle C (0.882 vs. 0.871), but when mapped to the r-θ plane, Nozzle C is slightly better than Nozzle B (0.9032 vs 0.9027).

References

[1] Chen H., Turbocharger turbine design by auto-optimisation. *Turbocharging Seminar 2013*, Tianjin, China, Sept. 2013.

[2] Chen H., Turbine wheel design for Garrett advanced variable geometry turbines for commercial vehicle applications. 8*th Int Conf on Turbochargers and Turbocharging;* Inst Mech Engrs; 2006.

[3] Yang D. F. et al., Investigations on the generation and weakening of shock wave in a radial turbine with variable guide vanes. *ASME Turbo Expo*, GT2016-57047.

[4] Zhan B. et al., Numerical Investigation of a novel approach for mitigation of forced response of a variable geometry turbine during engine braking mode. *ASME Turbo Expo*, GT2016-56342.

[5] Japikse D., Centrifugal compressor design and performance, Concepts ETI, Inc. 1996.

[6] Private conversation with Hideaki Tamaki of IHI Corp.